Appl. Phys. A (2014) 117:1885–1891
DOI 10.1007/s00339-014-8603-0

Applied Physics A
Materials Science & Processing

Side branch-based acoustic metamaterials with a broad-band negative bulk modulus

Chen Shen · Yun Jing

Received: 8 May 2014 / Accepted: 1 July 2014 / Published online: 10 July 2014

Abstract We present theoretical investigations and numerical simulations of one-dimensional (1-D) acoustic metamaterials that exhibit wide negative bulk modulus bands down to zero. The metamaterials consist of double or quadruple branch openings in a 1-D waveguide. A lumped model is developed for theoretical analysis and the bandwidths of negative bulk modulus for different structures are calculated and compared. As much as 100 % increase over the traditional single branch opening structure in bandwidth can be achieved. The proposed metamaterials can be utilized to further achieve double negativity, which could facilitate applications such as acoustic cloaking and superlensing.

1 Introduction

Acoustic metamaterials with negative effective parameters have received a great amount of attention in recent years since negativity is a key requirement in many novel applications of metamaterials, such as superlensing and cloaking [1–6]. In acoustic realm, common approaches to achieve negative bulk modulus can be divided into two categories: local-resonance type [7–9] and non-resonance type [10]. Local-resonance type approaches utilize locally resonance units such as Helmholtz resonators [7, 8] or split hollow spheres [9]. Due to the oscillating nature of the resonators, the bandwidth of negative modulus is narrow and cannot reach zero frequency. In addition, this type of negative bulk modulus is usually accompanied with strong energy dissipation. Lee et al. [10, 11] demonstrated that periodic structures with single branch openings are capable of producing negative modulus from zero frequency to a certain cutoff frequency. In their design, the negative bulk modulus was not introduced by resonance and consequently has low energy loss. In this paper, we propose a design of 1-D acoustic metamaterials with double and quadruple branch openings which have negative bulk modulus bands considerably wider than the ones with single branch openings. It also provides an alternative approach to tune the cutoff frequency and the effective bulk modulus of branch-based acoustic metamaterials. A lumped model was developed to predict the effective bulk modulus and the transmission coefficient of the metamaterial and the results agree well with the finite element simulation results. In addition, it is shown in this paper that, the end correction, which is an important parameter in the lumped model, can be derived using a combination of analytical and numerical solutions.

2 Theory

Figures 1a–c are schematics of single branch, double branch and quadruple branch opening metamaterials, respectively. The dimensions of the waveguide and branch openings are shown in Fig. 1d. The proposed metamaterials consist of unit cells with circular branch openings on the facades of each unit cell. All branches are assumed to have the same dimensions (i.e., height and radius). However, the analytical method outlined in this paper can be applied to more general cases. We here analyze the structures using a lumped model. In the equivalent acoustic transmission line circuit, a 1-D waveguide can be described by an acoustic compliance/capacitor in shunt and a mass/

C. Shen · Y. Jing (✉)
Department of Mechanical and Aerospace Engineering, North Carolina State University, Raleigh, NC 27695, USA
e-mail: yjing2@ncsu.edu

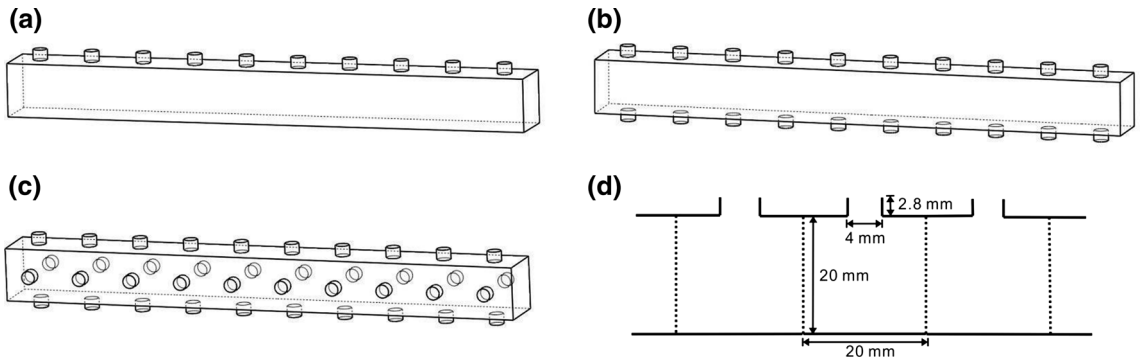

Fig. 1 Schematics of single branch and multiple branch opening metamaterials. **a** Single branch. **b** Double branch. **c** Quadruple branch. Ten unit cells are included in each structure. **d** The side view and dimensions of three unit cells with single branch openings

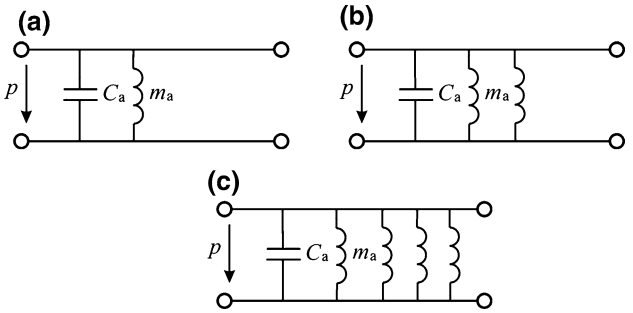

Fig. 2 Lumped model of the proposed structures. **a** Single branch. **b** Double branch. **c** Quadruple branch

inductor in series [12]. The inductor, however, only contributes to the effective density of the structure and is not included here for simplification. The branch openings, on the other hand, can be described by acoustic inductors in shunt [13] as shown in Fig. 2. The acoustic capacitance of the waveguide and the acoustic inductance of a single opening read

$$C_a = \frac{A}{E_0} d, \tag{1}$$

$$m_a = \frac{Z_a}{i\omega}, \tag{2}$$

where A is the cross-sectional area of the waveguide (square in this study), d is the length of the unit cell, $E_0 = \rho_0 c_0^2$ is the bulk modulus of the background medium, Z_a is the acoustic impedance of the branch at the inner opening connecting to the waveguide, ω is the angular frequency, and ρ_0 and c_0 are background medium density and sound speed, respectively. To this end, we will first estimate the total effective capacitance C_{eff} due to both C_a and m_a; the effective bulk modulus E_{eff} of the branch-based structures will then be derived by

$$C_{\text{eff}} = \frac{A}{E_{\text{eff}}} d. \tag{3}$$

For a single branch, the acoustic impedances at the two ends of the branch have the following relation [13]

$$Z_a = \frac{Z_0}{S} \frac{Z_{ah} S + i Z_0 \tan(k l_e)}{i Z_{ah} S \tan(k l_e) + Z_0}, \tag{4}$$

where $Z_0 = \rho_0 c_0$ is the acoustic impedance of the background medium, Z_{ah} is the acoustic impedance at the outer opening of the branch, S is the cross-sectional area of the branch opening, $k = \omega/c_0$ is the wave number, and l_e is the effective length of the branch. The effective length l_e is the sum of the height of the branch (h) and two end corrections for both inner and outer openings. Since the outer opening is unflanged, the end correction Δl_1 is theoretically $0.6 \times a$, where a is the radius of the openings [13]. There is no existing analytical end correction for the inner opening because it is connected to a confined space; the boundary condition is neither ideally flanged (of which the end correction is $0.85 \times a$) nor unflanged. The exact end correction for the inner opening, however, can be determined by numerical simulations and it is found that $\Delta l_2 = 0.69a$. Section III describes the detail on how this number was obtained. It is noted that accurate end corrections are critical in determining the cutoff frequency of the structure under study. They have not been discussed much, though, in the previous literatures on acoustic metamaterials. Furthermore, to model branches with opened ends, pressure release boundary condition ($Z_{ah} = 0$) was used and the branch height in the simulation was modified to be $h + \Delta l_1$. This is equivalent to modeling an opened branch with a height of h connecting to free space [14]. The acoustic impedance of the branch, i.e., Z_a, can then be simplified as:

$$Z_a = i \frac{\rho_0 c_0}{S} \tan(k l_e). \tag{5}$$

The effective total capacitance can be estimated from

$$\frac{1}{i\omega C_{\text{eff}}} = \frac{1}{i\omega C_a + Z_a^{-1}}. \tag{6}$$

As the unit size is significantly smaller than the wavelength at the frequency of interest, the structure can be regarded as a homogenized medium with an effective bulk modulus E_{eff}. Substituting Eqs. (1), (2) and (5) into Eqs. (6) and (3), we have

$$E_{\text{eff}} = \frac{\omega E_0}{\omega - \frac{SE_0}{\rho_0 c_0 Ad \tan(kl_e)}}. \tag{7}$$

At low frequencies, tan (kl_e) can be simplified tokl_e, and Eq. (7) reduces to

$$E_{\text{eff}} = \frac{\omega E_0}{\omega - \frac{SE_0}{\rho_0 c_0 Ad(kl_e)}}. \tag{8}$$

The cutoff frequency ω_0 for the single branch structure can be determined by setting the denominator in Eq. (8) to zero, which yields

$$\omega_0 = \left(\frac{Sc_0^2}{Adl_e}\right)^{1/2}. \tag{9}$$

Equations (8) and (9) show that, the bandwidth of negative modulus is determined by the cutoff frequency of the branch opening, i.e., the bulk modulus is negative below the cutoff frequency. We further consider acoustic metamaterials with double and quadruple branch openings. Because the acoustic inductors are in shunt as illustrated in Fig. 2b, c, the acoustic impedance of the branches are $Z_{\text{a}}^{\text{s}} = 2Z_{\text{a}}^{\text{d}} = 4Z_{\text{a}}^{\text{q}}$, where superscripts s, d and q represent single branch, double branch and quadruple branch openings, respectively. Equivalently, the effective lengths for different structures at low frequencies are $l_{\text{e}}^{\text{s}} = 2l_{\text{e}}^{\text{d}} = 4l_{\text{e}}^{\text{q}}$, due to the approximation to Eq. (5), i.e., $Z_{\text{a}} = i\frac{\rho_0 c_0}{S}(kl_{\text{e}})$. Substituting the resulting effective lengths into Eq. (9), the cutoff frequencies for different branch structures are

$$\omega_0^q = \sqrt{2}\omega_0^d = 2\omega_0^s. \tag{10}$$

Furthermore, for single branch opening metamaterials, the minimum value for l_{e} is $0.69 \times a + 0.85 \times a$, assuming h is infinitely small and the outer opening can be considered flanged. This will set an upper limit for the cutoff frequency ω_0 as

$$\omega_{0\max} = \left(\frac{Sc_0^2}{1.54Ada}\right)^{1/2}. \tag{11}$$

The minimum value for l_e can be now overcome using more branch openings, raising the upper bound for ω_0. Equations (10) and (11) imply that, within a frequency range of $\omega_0^s \sim 2\omega_0^s$, negative modulus can only be achieved by double branch or quadruple branch openings, provided that $\frac{S}{Ad}$ remains constant. It could be argued that increasing $\frac{S}{Ad}$ also raises the cutoff frequency. Geometrically, however, S is limited by the width of the waveguide (diameter cannot exceed the width), and d is also limited by the diameter of the opening (d cannot be less than the diameter). These pose bottlenecks for tuning the cutoff frequency. Utilizing multiple branch openings therefore provides an alternative means to increasing the cutoff frequency.

3 Computer modeling

Simulations were first carried out to determine the end correction Δl_2. Finite element software COMSOL 4.3b frequency-domain acoustic module was adopted. A model was established which involved one unit cell from the single branch opening structure (Fig. 3). The background medium properties and structure dimensions are listed in Table 1.

The transmission coefficient through this structure can be then computed at different frequencies. Two arbitrary frequencies within the bandwidth of interest were chosen: 100 and 400 Hz. Their transmission coefficients were 0.53 and 0.93, respectively. On the other hand, the analytical solution for the transmission coefficient of this structure can be written as [13]

$$T = 1 - \frac{Z_0/2A}{Z_0/2A + Z_{\text{a}}}, \tag{12}$$

where Z_{a} is given by Eq. (5) and depends on Δl_2. Figure 3 shows the transmission coefficients with varied Δl_2

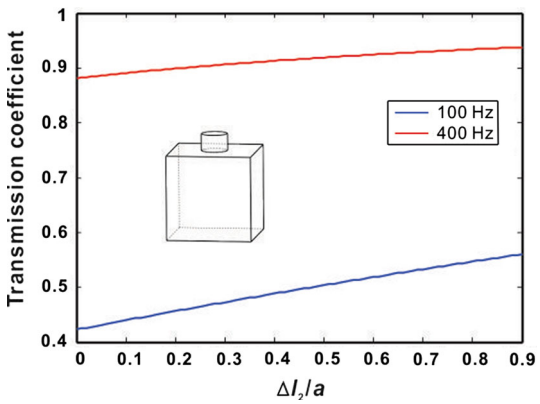

Fig. 3 Transmission coefficient for a unit cell with a single branch opening

Table 1 Background medium properties and structure dimensions used in the simulation

ρ_0 (kg/m^3)	c_0 (m/s)	r (mm)	h (mm)	d (mm)	A (mm^2)
1.2	343	2	2.8	20	400

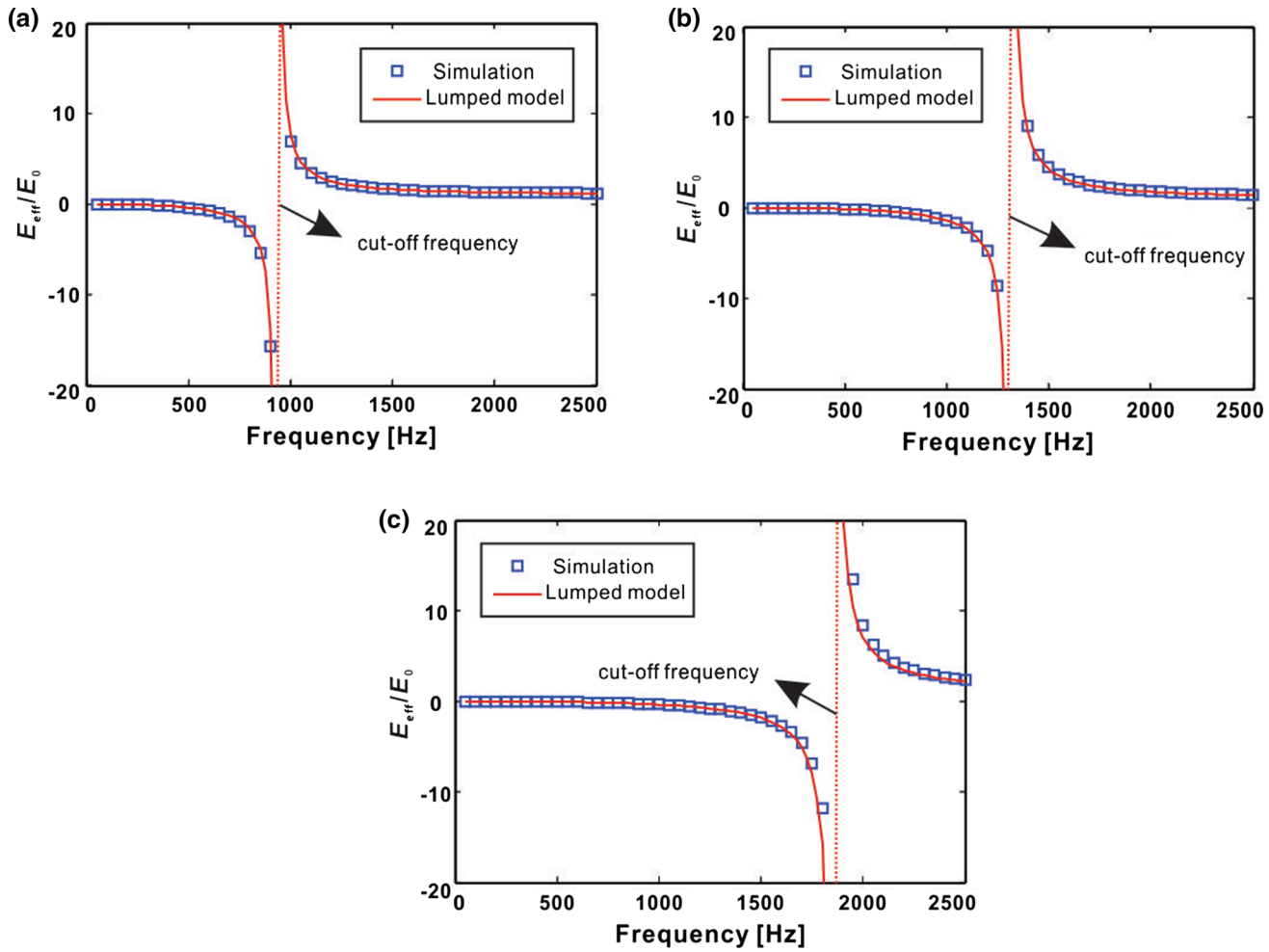

Fig. 4 Normalized bulk moduli of different branch structures. **a** Single branch opening. **b** Double branch opening. **c** Quadruple branch opening. The metamaterials have negative bulk moduli below cutoff frequencies where $E_{\text{eff}}/E_0 = 0$

predicted by Eq. (12). The theoretical values matched up with the COMSOL simulation results well when $\Delta l_2 = 0.69a$. This was used as the end correction for the inner opening of the branch throughout the paper. It must be stressed that, the end correction could depend on the geometry of the structure (e.g., cross-sectional areas of the waveguide and the branch) and therefore should be determined for the specific structure under study.

Subsequently, the lumped model was validated. COMSOL was used to compute the acoustic fields inside the proposed 1-D acoustic metamaterials depicted in Fig. 1. A finite-difference method was utilized to extract the effective bulk modulus from the acquired acoustic field [8, 15]. The normalized effective bulk modulus E_{eff}/E_0 of the 1-D acoustic metamaterials composed of single branch, double branch and quadruple branch openings are shown in Fig. 4a–c, respectively. Excellent agreement can be observed between theoretical and numerical approaches. The numerical results show that a single branch opening metamaterial has negative modulus below 930 Hz. The bandwidths of negative bulk modulus (or cutoff frequencies) obtained from simulations were 1,340 and 1,860 Hz for double branch and quadruple branch opening metamaterials, respectively. They are therefore 44 and 100 % higher than the traditional single branch opening design. According to Eq. (10), these two numbers in theory should be 41 and 100 % and they are in good agreement with simulation results. Our simulation and lumped model indicate that metamaterials with double or quadruple branch openings effectively broaden the negative bulk modulus band, owing to the reduced effective length of the branches. The effective bulk modulus of branch opening-based acoustic metamaterials can also be well predicted by the lumped model in the low frequency limit. It is noted that at the highest cutoff frequency, i.e., 1,860 Hz, the unit cell size (20 mm) is about 1/10 of the wavelength, justifying the usage of medium homogenization theory.

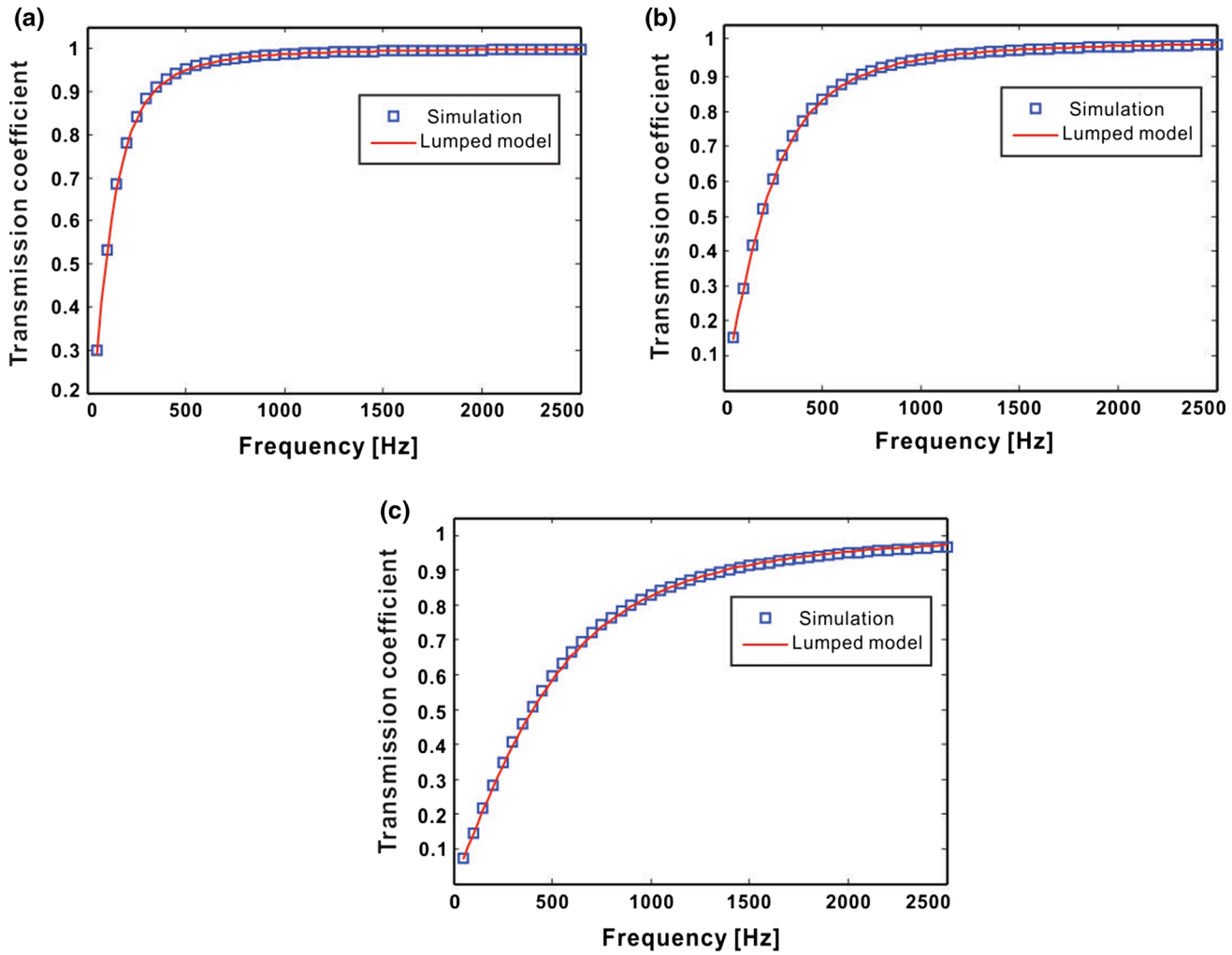

Fig. 5 Transmission coefficient for different structures with unit cell $n = 1$. **a** Single branch opening. **b** Double branch opening. **c** Quadruple branch opening

Finally, the transmission coefficients of the proposed metamaterials as homogenized media were investigated. The characteristic impedance of the metamaterial can be written as $Z_m = \rho_0 c_{eff}$, where $c_{eff} = \sqrt{\frac{E_{eff}}{\rho_0}}$ is the effective speed of sound. Consider a metamaterial layer of n unit cells with identical medium (air in this paper) on both sides, the reflection and transmission coefficients with normal incidence are [16]

$$R = \frac{Z_m^2 - Z_0^2}{Z_0^2 + Z_m^2 + 2iZ_0 Z_m \cot(\phi)}, \tag{13}$$

$$T = \frac{1 + R}{\cos(\phi) - \frac{Z_m i \sin(\phi)}{Z_0}}, \tag{14}$$

where $\phi = \frac{2\pi f n d}{c_{eff}}$ is the phase change across the layer, and Z_0 is the impedance of air. Figures 5 and 6 show the transmission coefficient against frequency predicted by Eq. (14), where Z_m was obtained by the lumped model. For comparison, numerical simulations using COMSOL were carried out again. To show the influence of the number of unit cells and validity of the lumped model for metamaterials at arbitrary lengths, two sets of results are shown, where n is equal to 1 and 10. Small ripples are observed above the cutoff frequencies, which indicate the coupling between unit cells. The transmission coefficient is also steeper as the number of unit cells increases. Ideally, an infinite number of unit cells will give a dramatic change of transmission coefficient at the cutoff frequency. However, the value of the cutoff frequency is not influenced by the number of unit cells, as it is intrinsically determined by the dimensions of the structures. The lumped model was able to accurately predict the transmission coefficient of the metamaterials under study. At $n = 10$, significant change of transmission coefficients can be observed: the stop-band of the acoustic metamaterial is significantly broadened using more branch openings.

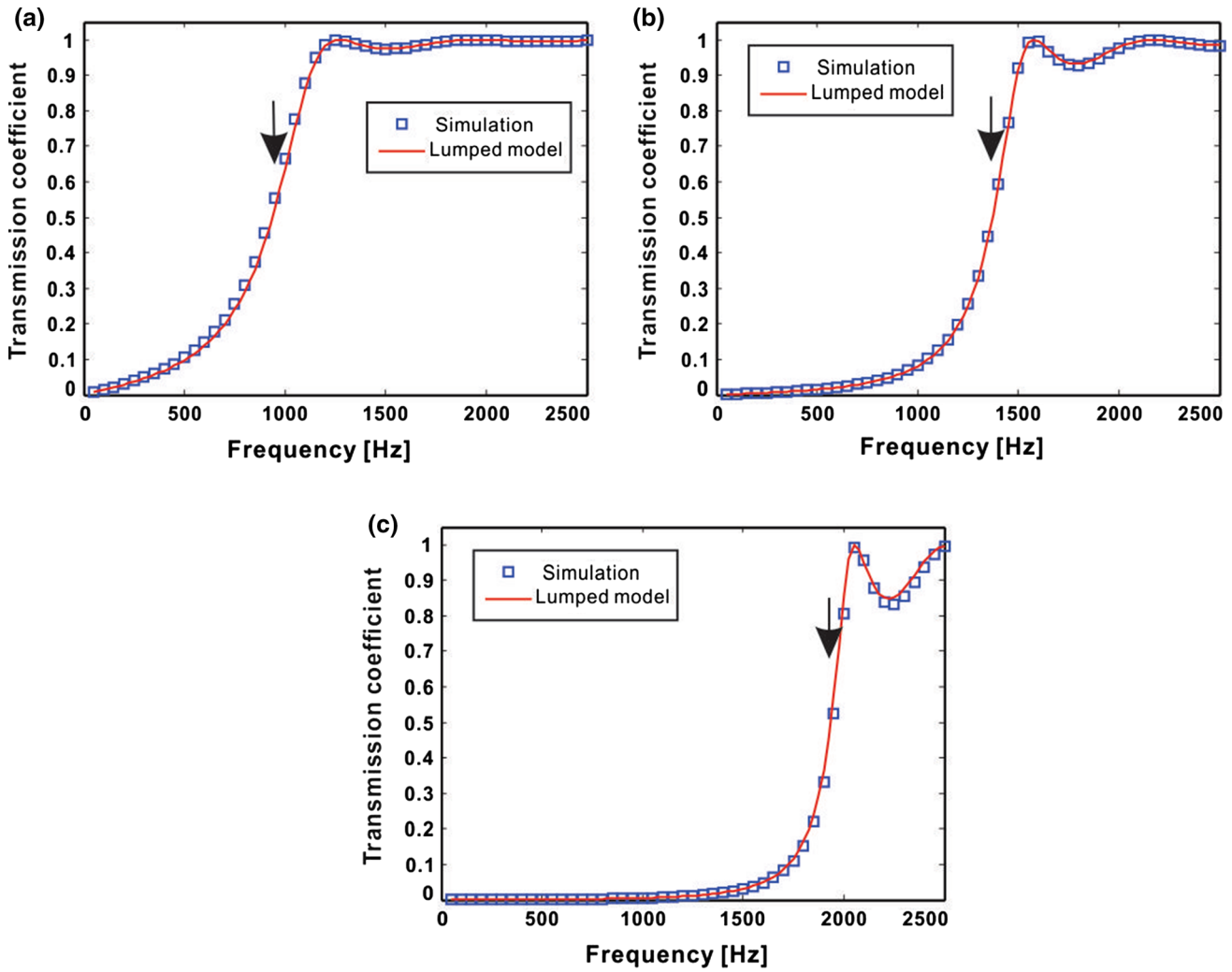

Fig. 6 Transmission coefficient for different structures with unit cells $n = 10$. The *arrows* indicate the cutoff frequencies predicted by Eq. 10. **a** Single branch opening. **b** Double branch opening. **c** Quadruple branch opening

4 Conclusions

To conclude, we provide theoretical analysis and full wave simulations of double branch and quadruple branch opening metamaterials. A lumped model is established to describe this type of acoustic metamaterials. The end correction for the branch opening is derived using a combination of analytical and numerical solutions. The comparison with the traditional single branch opening structure demonstrates that with multiple branch openings, the bandwidth of negative bulk modulus can be significantly broadened. The structure proposed here can be integrated with membrane-based metamaterials to achieve double negativity [11]. Double negativity is a key requirement for acoustic cloaking, complementary materials and superlens [1, 3, 7, 17]. We hope the broad bandwidth of the proposed structure can facilitate the design of these promising applications.

References

1. J. Pendry, Phys. Rev. Lett. **85**, 3966 (2000)
2. A. Grbic, G. Eleftheriades, Phys. Rev. Lett. **92**, 117403 (2004)
3. S. Zhang, L. Yin, N. Fang, Phys. Rev. Lett. **102**, 194301 (2009)
4. X. Zhou, G. Hu, Appl. Phys. Lett. **98**, 263510 (2011)
5. Y. Lai, J. Ng, H. Chen, D. Han, J. Xiao, Z.-Q. Zhang, C. Chan, Phys. Rev. Lett. **102**, 253902 (2009)
6. X. Zhu, B. Liang, W. Kan, X. Zou, J. Cheng, Phys. Rev. Lett. **106**, 014301 (2011)
7. N. Fang, D. Xi, J. Xu, M. Ambati, W. Srituravanich, C. Sun, X. Zhang, Nat. Mater. **5**, 452 (2006)
8. Y. Cheng, J. Xu, X. Liu, Phys. Rev. B **77**, 045134 (2008)
9. C. Ding, L. Hao, X. Zhao, J. Appl. Phys. **108**, 074911 (2010)
10. S.H. Lee, C.M. Park, Y.M. Seo, Z.G. Wang, C.K. Kim, J. Phys.: Condens. Matter **21**, 175704 (2009)
11. S.H. Lee, C.M. Park, Y.M. Seo, Z.G. Wang, C.K. Kim, Phys. Rev. Lett. **104**, 054301 (2010)
12. F. Bongard, H. Lissek, J.R. Mosig, Phys. Rev. B **82**, 094306 (2010)
13. L.E. Kinsler, A.U. Frey, A.B. Coppens, J.V. Sanders, *Fundamentals of Acoustics* (Wiley, New York, 1982)

14. A.D. Pierce, *Acoustics: An Introduction to Its Physical Principles and Applications* (Acoustical Society of America, New York, 1989)
15. S. Zhang, Acoustic Metamaterial Design and Applications (2010)
16. V. Fokin, M. Ambati, C. Sun, X. Zhang, Phys. Rev. B **76**, 144302 (2007)
17. H. Chen, C.T. Chan, J. Phys. D Appl. Phys. **43**, 113001 (2010)